

ON THE FORMATION OF ORTHO-BENZYNE ($o\text{-C}_6\text{H}_4$) UNDER SINGLE COLLISION CONDITIONS AND ITS ROLE IN INTERSTELLAR CHEMISTRY

FANGTONG ZHANG¹, DORIAN PARKER¹, Y. SEOL KIM¹, RALF I. KAISER¹, AND ALEXANDER M. MEBEL²

¹ Department of Chemistry, University of Hawai'i at Manoa, Honolulu, HI 96822, USA

² Department of Chemistry and Biochemistry, Florida International University, Miami, FL 33199, USA

Received 2010 October 12; accepted 2010 December 8; published 2011 February 1

ABSTRACT

The elementary reaction of the D1-ethynyl radical (C_2D) with vinylacetylene (C_4H_4) was studied under single collision conditions via crossed molecular beam experiments and electronic structure calculations. The results suggested that besides two acyclic isomers as predicted computationally, the ortho-benzyne ($o\text{-C}_6\text{H}_4$)—in its singly deuterated form—which is considered as an important intermediate in the formation of polycyclic aromatic hydrocarbons, can be formed in this process. This reaction was carried out at a collision energy of 40.9 kJ mol^{-1} , which is roughly equal to about 4000 K as present in photospheres of carbon stars and protoplanetary nebulae close to the central star. As the reaction is exoergic and involves no barriers higher than the separated reactants, our findings suggest that ortho-benzyne can also be formed in molecular clouds like TMC-1.

Key words: astrochemistry – ISM: molecules – methods: laboratory – molecular processes – planetary nebulae: individual (CRL-618)

Online-only material: color figures

1. INTRODUCTION

Since the very first postulation by Leger & Puget (1984) and Allamandola et al. (1985) as carbon-based matter in the interstellar medium, mounting evidence is suggesting that polycyclic aromatic hydrocarbons (PAHs) and related species like cationic, anionic, and partly (de)hydrogenated PAHs are the carriers of the unidentified infrared bands (UIRs) at 3.3, 6.2, 7.7, 8.6, 11.2, 12.7, and $16.4 \mu\text{m}$ (Peeters et al. 2002; Onaka 2004; Sakon et al. 2004; Tielens 2008; Onaka et al. 2009) and of the diffuse interstellar bands (DIBs) at 578.0, 579.7, 628.4, 661.4, and 443.0 nm (Halasinski et al. 2005; Hudgins et al. 2005; Sarre 2006; Cox et al. 2007; Joblin et al. 2009). Considering their chemical significance, PAHs could account for up to 30% of the cosmic carbon budget (Cook et al. 1996) and are also thought to play an important role in astrobiology (Allamandola & Hudgins 2003; Phillips & Parnell 2006; Alajtal et al. 2010). Due to their importance in the astrochemical evolution of the interstellar medium, Frenklach & Feigelson (1989) as well as Cherchneff et al. (1992) modeled the formation of PAHs in carbon-rich circumstellar envelopes. In these high-energy environments, where the circumstellar matter is exposed to an intense photon field from the central star, the chemistry is expected to be—with the exception of the lack of oxygen—similar to the high-temperature conditions as observed in combustion systems involving reactions of acetylene (C_2H_2), resonantly stabilized free radicals such as propargyl (C_3H_3), and the ethynyl radical (C_2H). These processes are also thought to involve hydrogen abstraction and acetylene addition (HACA) sequences (Bockhorn et al. 1987), phenyl addition steps, cyclization pathways (Shukla et al. 2008), and/or barrier-less ethynyl addition mechanisms (EAM; Mebel et al. 2008). Frenklach & Feigelson (1989) proposed a reaction scheme, in which carbenes such as vinylidene carbene (H_2CC) react with acetylene via vinylacetylene (C_4H_4) ultimately forming $o\text{-C}_6\text{H}_4$ via two successive atomic hydrogen losses. Sequential reactions with atomic hydrogen are suggested to lead to the formation of phenyl and benzene.

Among the growth species leading to PAH formation in these envelopes, the chemical properties and energetics of ortho-

benzyne ($o\text{-C}_6\text{H}_4$) have been thoroughly researched. Various gas-phase thermochemical data such as heats of formation (440 kJ mol^{-1} ; Rosenstock et al. 1980; Matimba et al. 1991) and ionization energies ($9.030 \pm 0.005 \text{ eV}$; Zhang & Chen 1992) are readily available. The infrared spectrum of $o\text{-C}_6\text{H}_4$ isolated in a low-temperature matrix was measured by several groups (Chapman et al. 1973; Dunkin & MacDonald 1979; Wentrup et al. 1988; Radziszewski et al. 1992). Its molecular structure in the gas phase was determined via microwave spectroscopy by Kukolich et al. (2004) and Robertson et al. (2003) to be a C_{2v} symmetric molecule. Photoelectron spectra (Zhang & Chen 1992) and the UV spectrum (Wenthold et al. 1996) of $o\text{-C}_6\text{H}_4$ were also studied to measure its singlet–triplet gap to be $160.9 \pm 10.0 \text{ kJ mol}^{-1}$ and $156.8 \pm 1.3 \text{ kJ mol}^{-1}$, respectively. Also, a few reactions of $o\text{-C}_6\text{H}_4$ were reported: Meier et al. (1998) suggested that $o\text{-C}_6\text{H}_4$ could add across five- or six-membered rings in the fullerene C_{70} . Zhang et al. (2007) studied the unimolecular thermal decomposition of $o\text{-C}_6\text{H}_4$. The authors found that at the threshold dissociation temperature of 1200–1400 K, it decomposes to form acetylene (C_2H_2) and diacetylene (C_4H_2) via a retro-Diels–Alder process.

Although significant works have been dedicated to the observation of PAHs and their aromatic building blocks in the interstellar medium, only benzene was proposed to exist in the protoplanetary nebula CRL-618 (Cernicharo et al. 2001). Previous chemical reaction models suggest that the phenyl radical and $o\text{-C}_6\text{H}_4$ likely co-exist with benzene (Frenklach & Feigelson 1989; Mebel et al. 2001; McMahan et al. 2003). Due to its larger dipole moment of 1.38D (Kraka & Cremer 1993) coupled with simpler spectroscopic structure compared to phenyl holding a dipole moment of only 0.9D (McMahan et al. 2003), $o\text{-benzene}$ ($o\text{-C}_6\text{H}_4$) is considered as a more likely candidate for detection toward CRL-618. In 2007, Widicus Weaver et al. (2007) conducted a search for $o\text{-benzyne}$ toward CRL-618 utilizing the Green Bank Telescope. Unfortunately, no transitions were detected; upper limits of the column density of $8.4 \times 10^{13} \text{ cm}^{-2}$ were determined. This result demonstrates the need for more studies on $o\text{-C}_6\text{H}_4$ -related chemistry since an understanding of the chemistry can guide astronomical searches in

Table 1

Peak Velocities (v_p) and Speed Ratios (S) of the Intersecting Segments of the Supersonic Beams Together with the Corresponding Collision Energies (E_c) and Center-of-mass Angles (Θ_{CM})

Beam	v_p (m s ⁻¹)	S	E_c (kJ mol ⁻¹)	Θ_{CM}
C ₂ D($X^2\Sigma^+$)	2080 ± 18	5.6 ± 0.4
C ₄ H ₄ (X^1A')	630 ± 20	25.0 ± 0.5	40.9 ± 0.3	31.2 ± 0.4

those regions of the interstellar medium where the proposed reactants have been detected or predicted by astrochemical models.

In this paper, we propose a route to form the D1-substituted form of o-benzyne under single collision conditions and provide experimental (via crossed molecular beams studies) and computational (via electronic structure calculations) evidence that the reaction of the D1-ethynyl radical (C₂D) with vinylacetylene (C₄H₄) can form—besides acyclic isomers—the D1-o-benzyne plus atomic hydrogen. Here, the ethynyl radical is a major photodissociation product of acetylene (Wodtke & Lee 1985; Jackson & Scodinu 2004), and the co-reagent—vinylacetylene—has been included in Frenklach & Feigelson’s (1989) model of circumstellar envelopes of carbon-rich stars. Our studies suggest that the bimolecular reaction of the ethynyl radical with vinylacetylene forms D1-o-benzyne (o-C₆H₄) via a similar reaction sequence involving addition and ring-closure processes that lead to the formation of the phenyl radical (C₆H₅) in the reaction of dicarbon molecules (C₂) with 1,3-butadiene (C₄H₆; Zhang et al. 2010).

2. EXPERIMENTAL

The reactive scattering experiments were conducted in a crossed molecular beams machine under single collision conditions at The University of Hawai’i (Gu et al. 2005a, 2005b; Guo et al. 2006a, 2006b). Briefly, a pulsed supersonic beam of deuterated ethynyl radicals in their electronic ground state (C₂D, $X^2\Sigma^+$) was generated in situ in the primary source chamber via laser ablation of graphite at 266 nm and a consecutive reaction of the ablated species with neat deuterium gas (99.995%; Icon). Deuterium also acted as a seeding gas of the ethynyl radicals. The pressure in the source chamber was maintained at 3×10^{-4} torr. The velocity and speed ratio of the reacting segment of the deuterated ethynyl radical beam were determined to be 2080 ± 18 m s⁻¹ and 5.6 ± 0.4 , respectively, after the beam passed a skimmer and a four-slot chopper wheel (Table 1). This part of the radical beam crossed a pulsed vinylacetylene beam (99.5%+) seeded in argon (99.9999%) at fractions of 5%. The traveling time of the primary beam between the ablation center and interaction region was about 20 μ s. Since the lifetime of the first electronically excited state, $A^2\Pi$, of ethynyl is less than 1 μ s, any C₂D($A^2\Pi$) species would relax to its ground electronic state while traveling from the ablation center to the interaction region. Vinylacetylene was synthesized according to the literature (Zhang et al. 2009). The segment of the vinylacetylene beam, which crossed the ethynyl radical beam, had a peak velocity and speed ratio of 630 ± 20 m s⁻¹ and 25.0 ± 0.5 , respectively. This resulted in a collision energy of 40.9 ± 0.6 kJ mol⁻¹ and a center-of-mass (CM) angle of 31.2 ± 0.4 . It is important to outline that the primary reactant beam also contained carbon atoms as well as dicarbon and tricarbon molecules. Previous studies of tricarbon reactions with acetylene, ethylene (Gu et al. 2007), and methylacetylene (Guo et al. 2007) suggest that tricarbon would have a significant entrance barrier

upon reacting with vinylacetylene; therefore, under our experimental conditions, tricarbon was not observed to react with vinylacetylene. The lighter carbon (12 amu) and dicarbon reactants (24 amu) react with vinylacetylene; due to the heavier ethynyl radical (26 amu), carbon and dicarbon reactions lead only to products which are lower in mass by 2 amu and 14 amu compared to those formed in the reaction of ethynyl radicals with vinylacetylene. Consequently, neither dicarbon nor carbon atoms interfered in the present study.

The reactively scattered products were monitored via a quadrupole mass spectrometric detector operating in the time-of-flight (TOF) mode at a constant mass-to-charge ratio (m/z) after electron-impact ionization of the molecules at 80 eV at an emission current of 2 mA. Up to 3.6×10^6 TOF spectra were recorded at each angle. The detector was rotatable within the plane defined by the ethynyl radical and vinylacetylene beams; this allowed the recording of angular resolved TOF spectra and—by integrating the TOF spectra at the laboratory angles—the laboratory angular distribution. The latter reported the integrated intensity of an ion of distinct m/z versus the laboratory angle. To gain additional information on the chemical dynamics and underlying reaction mechanism, the TOF spectra and laboratory angular distribution were fit and transformed into the CM reference frame using a forward-convolution routine (Vernon 1981; Weiss 1986). This approach initially presumed the angular flux distribution $T(\theta)$ and the translational energy flux distribution $P(E_T)$ in the CM system assuming mutual independence. The laboratory data (TOF spectra and the laboratory angular distribution) were then calculated from these $T(\theta)$ and $P(E_T)$ and convoluted over the apparatus functions to obtain a simulation of the experimental data. The output of this fitting routine is called the product flux contour map, $I(\theta, u) = P(u) \times T(\theta)$, which plots the intensity of the reactively scattered products (I) as a function of the CM scattering angle (θ) and product velocity (u) in the CM reference frame. This plot is called the reactive differential cross section and can be seen as an image of the chemical reaction.

3. THEORETICAL METHODS

Stationary points on the C₆H₄D doublet potential energy surface (PES) accessed by the reaction of ground-state D1-ethynyl radicals (C₂D) with vinylacetylene (C₄H₄), including the reactants, intermediates, transition states, and possible products, were optimized at the hybrid density functional B3LYP level with the 6–311G** basis set (Lee et al. 1988; Becke 1993). Vibrational frequencies were calculated using the same B3LYP/6–311G** method and were used to compute zero-point vibrational energy (ZPE) corrections. Relative energies of various species were refined employing the coupled cluster CCSD(T) method (Purvis & Bartlett 1982; Pople et al. 1987; Scuseria et al. 1988; Scuseria & Schaefer 1989) with Dunning’s correlation-consistent cc-pVDZ and cc-pVTZ basis sets (Dunning 1989). Then the total energies were extrapolated to the complete basis set (CBS) limit using the equation $E_{\text{total}}(\text{CBS}) = (E_{\text{total}}(\text{VTZ}) - E_{\text{total}}(\text{VDZ}) \times 2.5^3/3.5^3)/(1 - 2.5^3/3.5^3)$ (Huh & Lee 2003). In order to evaluate reaction energies more accurately, we carried out CCSD(T) calculations for the most important products with a larger cc-pVQZ basis set and extrapolated their CCSD(T)/CBS total energies from the CCSD(T)/cc-pVDZ, CCSD(T)/cc-pVTZ, and CCSD(T)/cc-pVQZ values using the following formula, $E_{\text{tot}}(x) = E_{\text{tot}}(\infty) + Be^{-Cx}$, where x is the cardinal number of the basis set (2–4) and $E_{\text{tot}}(\infty)$ is the CCSD(T)/CBS

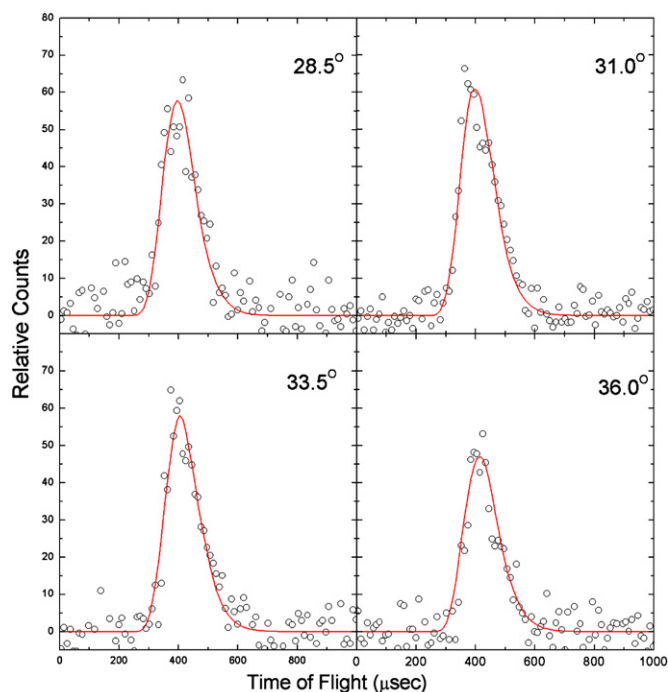


Figure 1. Selected TOF spectra recorded at $m/z = 77$ ($C_6H_3D^+$) at various laboratory angles for the reaction of the deuterated ethynyl radical with vinylacetylene at a collision energy of 40.9 kJ mol^{-1} . The circles indicate the experimental data, and the solid lines the calculated fits from the one channel fit.

(A color version of this figure is available in the online journal.)

total energy (Peterson & Dunning 1995). Relative energies discussed in the paper are thus computed at the CCSD(T)/CBS//B3LYP/6-311G** + ZPE(B3LYP/6-311G**) level of theory with two-point CBS extrapolation for all intermediates and transition states and three-point extrapolation for the significant products. All quantum-chemical calculations were performed utilizing the GAUSSIAN 98 (Frisch et al. 2001) and MOLPRO (Amos et al. 2003) program packages. The results of the ab initio calculations, such as relative energies and molecular parameters, were utilized in RRKM calculations of energy-dependent rate constants, which in turn were used to compute product branching ratios at different collision energies (Kislov et al. 2004).

4. RESULTS

4.1. Laboratory Data

Signal was monitored for $m/z = 77$ and 76 corresponding to ions with the molecular formula $C_6H_3D^+$ ($m/z = 77$) and $C_6H_4^+$ and/or $C_6H_2D^+$ ($m/z = 76$). Since the primary beam also contained dicarbon molecules, which also reacted with molecules containing carbon-carbon double or triple bonds (Balucani et al. 2001; Kaiser et al. 2003), we did not record TOF spectra at mass-to-charge ratio of $m/z = 75$ ($C_6H_3^+$) and below. It shall be stressed that after scaling, TOF spectra recorded at $m/z = 76$ were superimposable with those recorded at $m/z = 77$. Therefore, these raw data alone suggest that a molecule of the formula C_6H_3D represented the reaction product via a D1-ethynyl versus atomic hydrogen exchange pathway. Further, the ions at $m/z = 76$ were formed via dissociative ionization of the parent molecule in the electron impact ionizer; also, this finding is indicative that neither a molecular hydrogen loss nor an atomic deuterium loss pathway contributed to the signal at

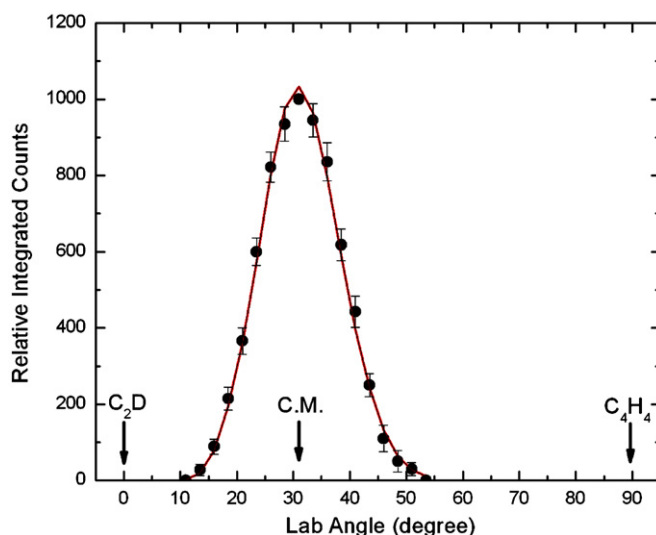


Figure 2. Laboratory angular distribution (LAB) of the C_6H_3D product recorded at $m/z = 77$ ($C_6H_3D^+$) at a collision energy of 40.9 kJ mol^{-1} for the reaction of the deuterated ethynyl radical with vinylacetylene. Circles and error bars indicate experimental data, and the solid line the calculated distribution with the one channel best-fit CM functions.

(A color version of this figure is available in the online journal.)

$m/z = 76$. This presents a crucial finding when we elucidate the underlying reaction mechanism(s). Consequently, only the D1-ethynyl versus atomic hydrogen exchange pathway is open within this mass range, but pathways involving deuterium and/or molecular hydrogen loss were closed under our experimental conditions. Due to the highest signal-to-noise ratio, all the TOF spectra were taken at $m/z = 77$. The TOF spectra and their corresponding laboratory angular distribution are shown in Figures 1 and 2. Note that the laboratory angular distribution is relatively narrow and spreads only over 40° within the scattering plane. Further, the laboratory angular distribution peaks close to the CM angle of the deuterated ethynyl–vinylacetylene system. These results suggest that the reaction likely proceeds via indirect scattering dynamics.

4.2. Center-of-mass Angular, $T(\theta)$, and Translational Energy, $P(E_T)$, Distributions

We were able to fit the recorded TOF spectra (Figure 1) and laboratory angular distribution (Figure 2) at $m/z = 77$ ($C_6H_3D^+$) with a single channel of the product mass combination 77 amu (C_6H_3D) plus 1 (H) amu by utilizing a parameterized CM angular distribution and a CM translational energy distribution in point form. The derived CM functions are shown in Figure 3. The CM angular distribution, $T(\theta)$, depicts intensity over the complete angular range from 0° to 180° ; further, within the error limits, all fits were forward–backward symmetric with respect to 90° . The best fits were achieved with an isotropic (flat) function, though within the error limits, fits with either a small maximum or shallow minima at 90° were also feasible. These findings indicate that the D1-ethynyl–vinylacetylene reaction involves indirect scattering dynamics via the formation of bound C_6H_4D reaction intermediate(s) (Levine 2005). Also, the inherent forward–backward symmetry of the $T(\theta)$ suggests that the lifetime of the intermediate(s) is longer than its (their) rotational period (Miller et al. 1967) or that the intermediate is “symmetric” (Kaiser et al. 1996). In the latter case, a rotational axis of the decomposing intermediate would interconvert two hydrogen atoms; this leads to an emission of atomic hydrogen

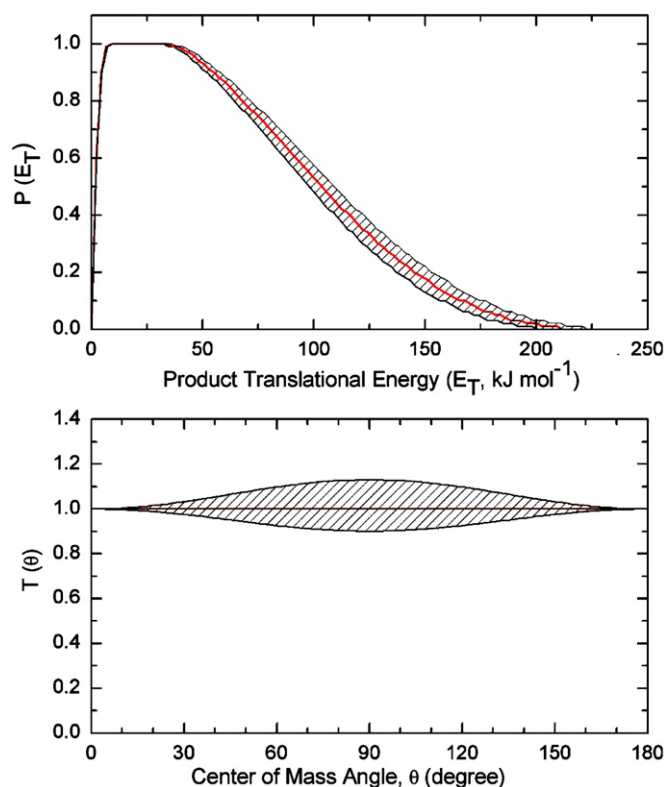


Figure 3. One channel fit: center-of-mass angular (top) and translational energy flux distributions (bottom) of the C_6H_3D plus atomic hydrogen channel of the reaction of deuterated ethynyl radical with vinylacetylene. Hatched areas indicate the acceptable upper and lower error limits of the fits. The red line defines the best-fit functions.

(A color version of this figure is available in the online journal.)

with equal probability into θ° and $\pi - \theta^\circ$ thus resulting in a forward-backward symmetric CM angular distribution. It should also be noted that the lack of polarization of the CM angular distribution can be explained by poor coupling between the initial and the final orbital angular momentum and the emission of a light hydrogen atom (Miller et al. 1967). Angular momentum conservation dictates that in this case, most of the initial orbital angular momentum is channeled into the rotational excitation of the polyatomic C_6H_3D product.

The CM translational energy distribution, $P(E_T)$, provides us with additional information on the reaction dynamics. For this system, $P(E_T)$ extends up to a maximum translational energy of 208 kJ mol^{-1} (Figure 3). Adding or subtracting 20 kJ mol^{-1} does not change the fit significantly. Since the high-energy cutoff presents the sum of the absolute reaction energy and the collision energy, we can subtract the collision energy to compute the reaction energy to be exoergic by $167 \pm 20 \text{ kJ mol}^{-1}$. Second, the $P(E_T)$ is fairly broad and displays a distribution plateau from close to zero translational energy to about 35 kJ mol^{-1} . This finding suggests the existence of at least two reaction pathways, one of them holding a tight exit barrier upon decomposition of the C_6H_4D intermediate(s). This pattern has also been observed, for instance, in the reactions of ground-state singlet and first excited-state triplet dicarbon with unsaturated hydrocarbon molecules (Gu et al. 2006). Here, reactions of singlet dicarbon result ultimately in reaction intermediates fragmenting via simple bond rupture and hence lose exit transition states, whereas on the triplet surface, tight exit transition states dictate the reaction dynamics (Kaiser et al. 2010). Finally, by integrating the CM translational energy

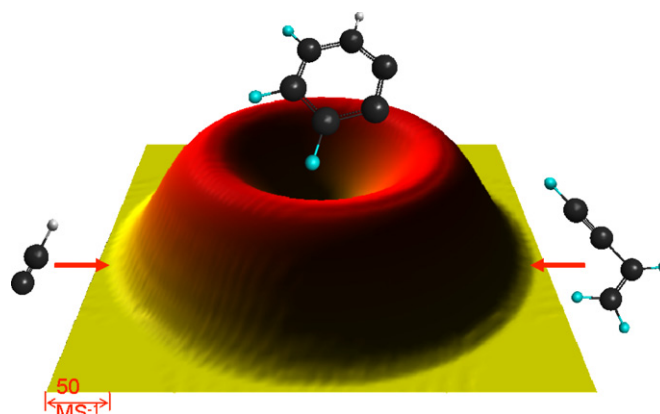


Figure 4. Flux contour map of the reaction of the deuterated ethynyl radical with vinylacetylene to form C_6H_3D and atomic hydrogen at a collision energy of 40.9 kJ mol^{-1} .

(A color version of this figure is available in the online journal.)

distribution and accounting for the available energy, the average fraction of available energy channeling into the translational degrees of freedom is computed to be $29.8 \pm 0.3\%$. This order of magnitude indicates indirect scattering dynamics via complex formation as already predicted from the laboratory and CM angular distributions. Figure 4 also compiles the flux contour map of this one channel fitting.

4.3. Computational Results

In the case of complex reaction systems, it is always useful to merge the experimental data with electronic structure calculations. Hence we also carried out high-level ab initio calculations of the ethynyl-vinylacetylene reaction on the doublet C_6H_5 PES. The calculation revealed that eight distinct C_6H_4 isomers (**p1**–**p8**, Figure 5) can be formed with the aromatic D1-o-benzyne molecule (**p6**) plus atomic hydrogen being the most exoergic reaction pathway (-167 kJ mol^{-1}). A group of five isomers (**p1**, **p3**, **p5**, **p7**, **p8**) are less stable by about 50 – 65 kJ mol^{-1} ; **p2** and **p4** are the least stable isomers. Our calculations also revealed that the formation of the products strongly depended on the position in the vinylacetylene molecule where the initial attack of the ethynyl radical occurs. There are four scenarios: (1) attack to the terminal acetylenic carbon (Figure 6(a)); (2) attack to the terminal ethylenic carbon (Figure 6(b)); (3) attack to the inner acetylenic carbon (Figure 6(c)); and (4) attack to the inner ethylenic carbon (Figure 6(c)). Below, the computational results will be discussed in this order.

1. The ethynyl radical can add to the terminal acetylenic carbon atom without entrance barrier to form a doublet reaction intermediate **i1** which is $284.9 \text{ kJ mol}^{-1}$ below the separated reactants. Note that hereafter, all the energetics are given relative to the separate reactants, unless otherwise noted. From **i1**, the addition complex can undergo hydrogen atom emission to either **p1** vinylidiacetylene or **p2** hexa-1,2,3-triene-5-yne. The **p1** pathway has an exoergicity of $-123.8 \text{ kJ mol}^{-1}$ with an exit barrier of 20.9 kJ mol^{-1} ; the **p2** pathway, on the other hand, has an exoergicity of $-75.7 \text{ kJ mol}^{-1}$ with an exit barrier of 18.8 kJ mol^{-1} . Alternatively, **i1** can undergo a ring closure to form a bicyclic intermediate **i2**; the latter can either lose a hydrogen atom overcoming a barrier of $113.4 \text{ kJ mol}^{-1}$ to form **p3** m- C_6H_4 which has an exoergicity of $-121.8 \text{ kJ mol}^{-1}$; alternatively

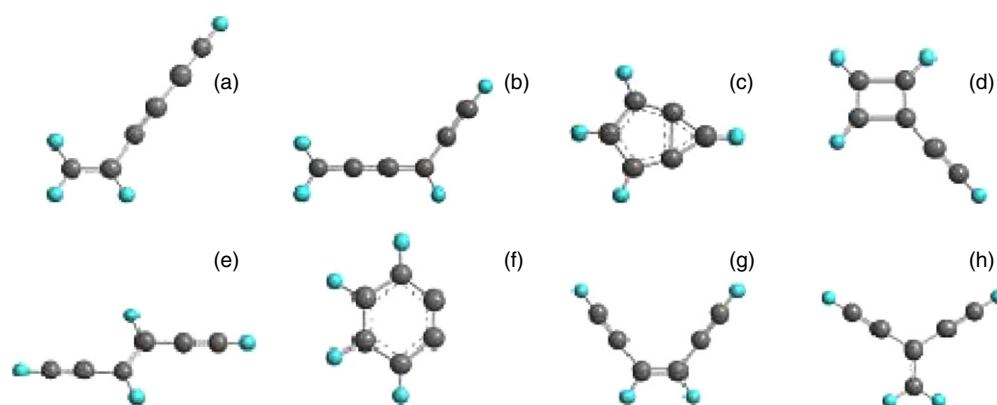


Figure 5. Structures and energies of possible C_6H_4 products. Relative energies are calculated at the CCSD(T)/CBS level with three point extrapolation in parentheses. (a) **p1**: vinylidiacetylene (-123.8 kJ mol $^{-1}$). (b) **p2**: hexa-1,2,3-triene-5-yne (-75.7 kJ mol $^{-1}$). (c) **p3**: m-benzyne (-121.8 kJ mol $^{-1}$). (d) **p4**: c- $C_4H_3(C_2H)$ (18.4 kJ mol $^{-1}$). (e) **p5**: (E)-hexa-3-ene-1,5-diyne (-113.3 kJ mol $^{-1}$). (f) **p6**: ortho-benzyne (-181.6 kJ mol $^{-1}$). (g) **p7**: (Z)-hexa-3-ene-1,5-diyne (-113.8 kJ mol $^{-1}$). (h) **p8**: diethynylethene (-103.3 kJ mol $^{-1}$).

i2 can overcome a significant barrier of 221.3 kJ mol $^{-1}$ to form a six-membered single ring intermediate **i10**, which has a relative energy of -179.9 kJ mol $^{-1}$ to the separated reactants. Intermediate **i10** then overcomes a barrier of 48.5 kJ mol $^{-1}$ and isomerizes via hydrogen migration to form **i8**—the phenyl radical. This intermediate represents the global energy minimum of this part of the C_6H_5 PES, which is 515.9 kJ mol $^{-1}$ below the separate reactants. **i8** can emit a hydrogen atom, without any barrier, to form **p6** D1-ortho-benzyne with an overall exoergicity of -181.6 kJ mol $^{-1}$. The third pathway from **i2** involves hydrogen migration through a barrier of 141.4 kJ mol $^{-1}$ to form intermediate **i6** which is located 190.4 kJ mol $^{-1}$ below the reactants. The latter can undergo yet another hydrogen migration, this time over a barrier of 115.1 kJ mol $^{-1}$, to form intermediate **i9**. Intermediate **i9** then ring opens to the phenyl radical, **i8** via a transition state located at -250.6 kJ mol $^{-1}$. Ultimately, **i8** then loses a hydrogen atom to form **p6** D1-ortho-benzyne as described above. From **i1**, a fourth pathway involves hydrogen migration. Over a barrier of 225.1 kJ mol $^{-1}$, an acyclic intermediate **i3** is formed from **i1**. The latter then undergoes rotation around a single C–C bond through a small barrier of only 24.3 kJ mol $^{-1}$ to form intermediate **i4**. Both **i3** and **i4** can access **p5**, (E)-hexa-3-ene-1,5-diyne, via hydrogen atom loss through barriers located at -91.6 and -89.1 kJ mol $^{-1}$, respectively. This reaction pathway has an exoergicity of -113.3 kJ mol $^{-1}$. Besides the hydrogen atom loss pathway, **i4** can also undergo ring closure via a transition state located at -133.9 kJ mol $^{-1}$ to form a four-membered ring intermediate **i5**. This intermediate can emit a hydrogen atom to form **p4** c- $C_4H_3(C_2H)$ without an exit barrier. Alternatively, **i5** ring opens to form intermediate **i7**. This process has a significant barrier of 169.9 kJ mol $^{-1}$. The **i7** intermediate can either lose a hydrogen atom over a barrier of 155.2 kJ mol $^{-1}$, to form **p7** (Z)-hexa-3-ene-1,5-diyne or can undergo a ring-closure process through a barrier of 20.5 kJ mol $^{-1}$, to form **i8** and then **p6** plus hydrogen as described above.

2. The ethynyl radical can also add to the terminal ethylenic carbon without an entrance barrier to form the addition complex **i11**, which is stabilized by 271.5 kJ mol $^{-1}$. From **i11**, there are three possible pathways. The first of which is an atomic hydrogen emission. Overcoming a

barrier located at -98.3 kJ mol $^{-1}$, **i11** emits a hydrogen atom to form **p7** (Z)-hexa-3-ene-1,5-diyne. The second pathway involves a ring closure which is accessed by overcoming a barrier of 127.2 kJ mol $^{-1}$; **i11** closes to form a six-membered ring **i12**. The latter then overcomes a barrier of 48.5 kJ mol $^{-1}$ and a subsequent hydrogen migration to form **i8**, the phenyl radical. The phenyl radical, **i8**, then emits a hydrogen atom without any barrier to form **p6** D1-ortho-benzyne in an overall exoergic process (-181.6 kJ mol $^{-1}$). The third pathway from **i11** involves a hydrogen migration, overcoming a barrier located at -69.9 kJ mol $^{-1}$, to yield intermediate **i7**. This structure then either emits atomic hydrogen to access **p7** (Z)-hexa-3-ene-1,5-diyne, or undergoes a ring closure to form **i8** phenyl and subsequently **p6** D1-ortho-benzyne plus a hydrogen atom as described above. This process has a barrier located at -223.8 kJ mol $^{-1}$.

3. The ethynyl radical attacks the middle acetylenic carbon to form intermediate **i14**, which can dissociate, overcoming a barrier located at -71.1 kJ mol $^{-1}$, to form C_2H_3 and C_4H_2 . This reaction has an exoergicity of 99.6 kJ mol $^{-1}$. Alternatively, **i14** can ring close, via a transition state located at -142.7 kJ mol $^{-1}$, to form a three-membered ring intermediate **i15**. The latter then ring opens over a barrier of 27.2 kJ mol $^{-1}$ to access intermediate **i1** located at -284.9 kJ mol $^{-1}$. Thus, the migration of the C_2H group in **i14**, **i14** \rightarrow **i15** \rightarrow **i1**, is much more favorable than the dissociation of this adduct. This ethynyl group migration leads to **i1**, which is the initial complex of ethynyl addition to the terminal acetylenic carbon, and therefore the ethynyl addition to the middle acetylenic carbon is likely to access that same area of the PES as the terminal addition (Figure 6(a)).
4. The attack of the ethynyl radical to the central ethylenic carbon will result in the formation of **i13** without any barrier. This intermediate is located at -211.3 kJ mol $^{-1}$. **i13** can then lose a hydrogen atom by overcoming a barrier located at -69.5 kJ mol $^{-1}$ to form **p8** diethynylethene with an exoergicity of -103.3 kJ mol $^{-1}$. Alternatively, **i13** can isomerize to **i11** by C_2H migration via a three-membered ring intermediate **i16** and two transition states residing at -177.0 , -141.4 , and -166.9 kJ mol $^{-1}$, respectively. We can conclude that the **i13** \rightarrow **i16** \rightarrow **i11** rearrangement is significantly more preferable than the dissociation of

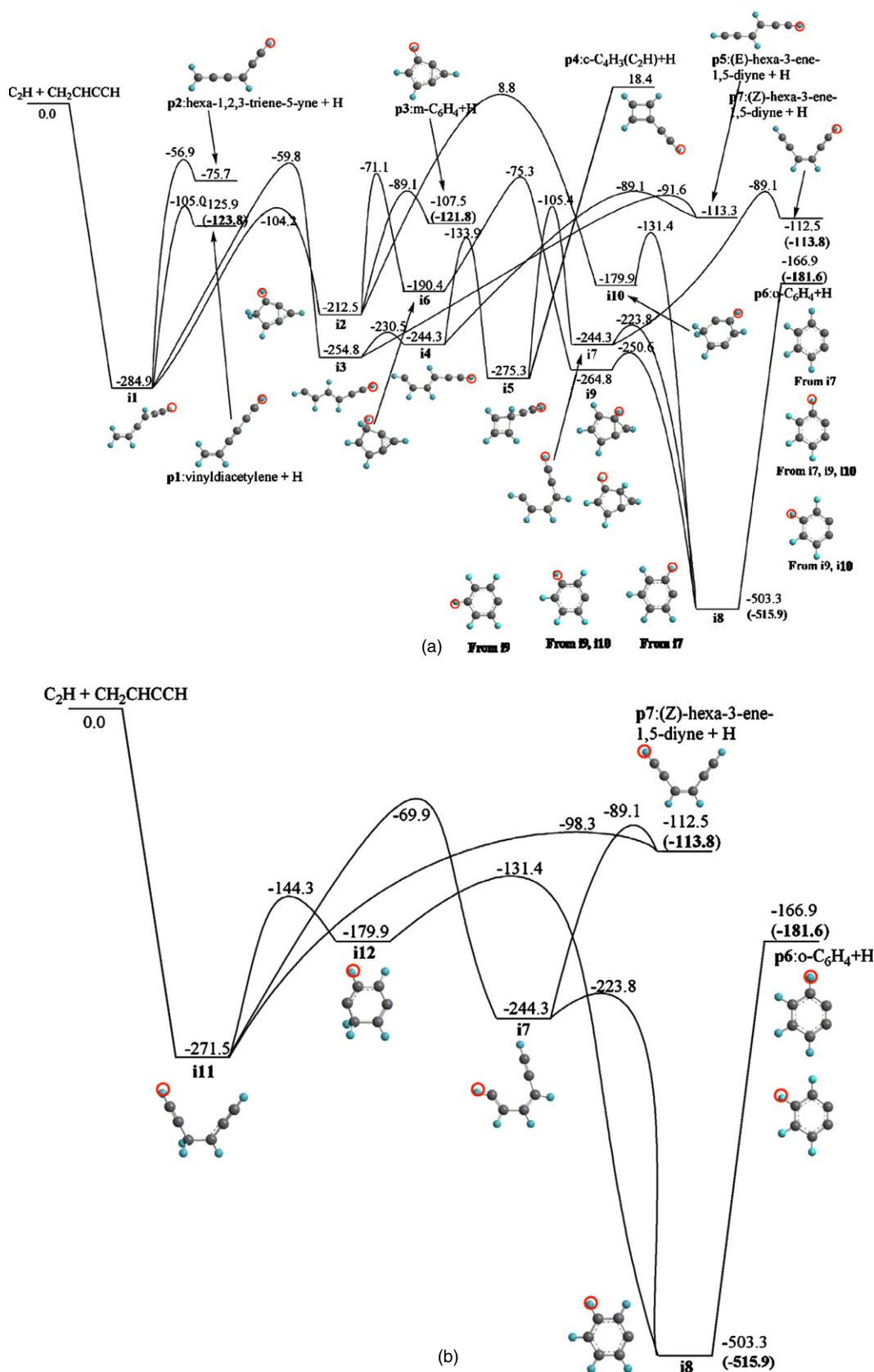


Figure 6. Potential energy surfaces of the reaction of the ethynyl radical and vinylacetylene. Circled atoms are the deuterium atom position for the deuterated ethynyl radical. Relative energies are calculated at the CCSD(T)/CBS level with two-point extrapolation (in parentheses, with three-point extrapolation) and given in kJ mol^{-1} . Energies of the D1-substituted reactants, intermediates, and products differ in zero-point energies by less than 5 kJ mol^{-1} .

(A color version of this figure is available in the online journal.)

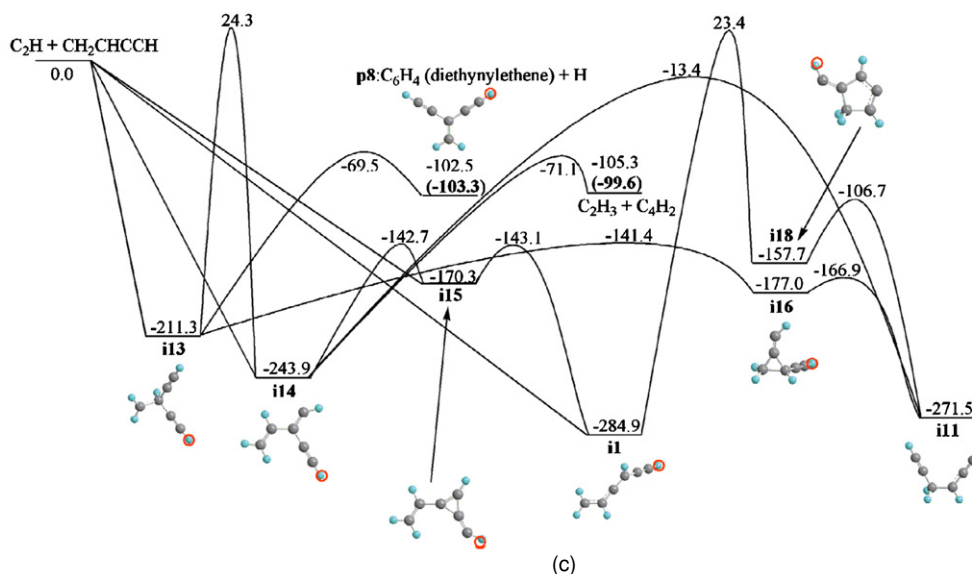


Figure 6. (Continued)

i13 and therefore the central ethylenic addition would likely access the same area of the surface as the terminal ethylenic addition. On the other hand, the alternative ethynyl migrations, **i13** → **i14**, **i14** → **i11**, and **i1** → **i11**, which would merge the acetylenic and ethylenic addition reaction pathways, are not likely to occur due to much higher barriers.

5. DISCUSSION

Now we are combining both the experimental and computational results in an attempt to untangle the reaction dynamics of the ethynyl–vinylacetylene system. First, let us compile the experiment results.

1. Under our experimental conditions, only a product of a formula C_6H_3D was detected, which suggested that the D1-ethynyl versus atomic hydrogen exchange was the only open pathway. The emitted hydrogen atom must therefore come from the vinylacetylene molecule.
2. The best-fit CM angular distribution (isotropic) indicated that this reaction was governed by indirect scattering dynamics, and proceeded via a long-lived intermediate(s) with a general formula of C_6H_4D . This mechanism was further verified by the CM translational energy distribution, where only about 30% of the total available energy channeled into the translational mode of freedom.
3. The CM translational energy distribution revealed that the reaction to form C_6H_3D plus atomic hydrogen is exoergic by $167 \pm 20 \text{ kJ mol}^{-1}$.

Having summarized the experimental findings, the next step is to identify the product(s) formed in the reaction of D1-ethynyl with vinylacetylene. Based on this information we can then connect the structures of the reactant with the products and utilize the data on the dynamics to unravel the actual reaction pathway(s). A comparison of the experimentally derived reaction exoergicities with the computational results (Figure 5) reveals that at least **p6** (D1-ortho-benzynes) presents the product. The experimental and computational results show a close match: D1-ortho-benzynes is the only product which can account for the high (167 kJ mol^{-1}) reaction exoericity within the error limits.

The identification of D1-o-benzynes leads us now to the investigation of the reaction pathway. Based on the calculations, D1-o-benzynes is formed only via a barrier-less hydrogen loss from the phenyl radical (**i8**). The barrier-less nature of a decomposing intermediate was predicted based on the CM translational distribution of this channel peaking close to zero translational energy. Considering the structure of phenyl versus D1-o-benzynes, the emitted hydrogen atom must be in the ortho position with respect to the radical center in the phenyl radical. Further, the experiments predict that only a hydrogen atom can be lost, but not a deuterium atom; the deuterium atom from the D1-ethynyl reactant is incorporated in the D1-o-benzynes molecule. In principle, four reaction pathways can lead to o-benzynes:

1. reactants → **i1** → **i2** → **i10** → **i8** → **p6** + H,
2. reactants → **i1** → **i2** → **i6** → **i9** → **i8** → **p6** + H,
3. reactants → **i1** → **i3** → **i4** → **i5** → **i7** → **i8** → **p6** + H,
4. reactants → **i11** → **i7/i12** → **i8** → **p6** + H.

Which is the actual pathway to form o-benzynes? The pathway reactants → **i1** → **i3** → **i4** → **i5** → **i7** → **i8** → **p6** + H can be excluded since in the phenyl radical, both a hydrogen and a deuterium atom are located on both ortho positions with respect to the radical center. However, a deuterium loss was not observed experimentally. Both reaction sequences (1) and (2) can account for the experimental findings: pathway (1) leads to a D1-substituted phenyl radical **i8** with the deuterium atom at the meta position with respect to the radical center; sequence (2) involves a hydrogen migration from **i2** to **i6**, in which the deuterium and hydrogen atoms are connected to the methylene unit. Here, a hydrogen or deuterium migration can lead to two distinct intermediates **i9**, which in turn lead to **i8** structures in which the deuterium atom is in meta or para position with respect to the radical center. Therefore, both ortho and meta radical centers can emit only a hydrogen atom from the ortho position with respect to the thus explaining the experimentally observed atomic hydrogen elimination pathway. Comparing pathways (1)–(3), all three reactions involve the intermediate **i1**. The inherent barriers of **i1** to isomerize to **i3** and **i2** of $205.0 \text{ kJ mol}^{-1}$ and $108.3 \text{ kJ mol}^{-1}$, respectively, lead us to the

Table 2
Product Branching Ratios (%) Calculated at Different Collision Energies under Single Collision Conditions

Ethynyl Addition to the Terminal Acetylenic Carbon (Starting from i1)								
Products	Collision Energy (kJ mol ⁻¹)							
	0	4.2	8.4	12.6	16.7	20.9	30.0	40.9
p1	97.74	97.52	97.21	96.93	96.63	96.28	95.54	94.76
p2	0.08	0.10	0.12	0.15	0.17	0.20	0.28	0.38
p3	0.32	0.30	0.29	0.28	0.27	0.26	0.24	0.22
p6	0.01	0.01	0.01	0.01	0.01	0.01	0.01	0.01
C ₂ H ₃ +C ₄ H ₂	1.85	2.06	2.36	2.63	2.92	3.24	3.93	4.63
Ethynyl Addition to the Middle Acetylenic Carbon (Starting from i14)								
Products	Collision Energy (kJ mol ⁻¹)							
	0	4.2	8.4	12.6	16.7	20.9	30.0	40.9
p1	97.07	96.67	96.16	95.64	95.07	94.39	92.77	90.89
p2	0.08	0.10	0.12	0.15	0.17	0.20	0.27	0.36
p3	0.31	0.30	0.29	0.27	0.26	0.25	0.23	0.21
p6	0.01	0.01	0.01	0.01	0.01	0.01	0.01	0.01
C ₂ H ₃ +C ₄ H ₂	2.52	2.92	3.42	3.93	4.48	5.14	6.71	8.53
Ethynyl Addition to the Terminal Ethylenic Carbon (Starting from i11)								
Products	Collision Energy (kJ mol ⁻¹)							
	0	4.2	8.4	12.6	16.7	20.9	30.0	40.9
p7 from i11	88.80	89.72	90.48	91.12	91.69	92.09	92.88	93.38
p7 from i7	0.00	0.00	0.00	0.00	0.00	0.00	0.01	0.01
p7 total	88.80	89.72	90.48	91.12	91.69	92.09	92.89	93.39
p6 via i12	9.84	8.78	7.87	7.08	6.37	5.81	4.66	3.81
p6 via i7	0.91	0.99	1.07	1.15	1.24	1.32	1.51	1.70
p6 total	10.75	9.77	8.94	8.24	7.60	7.12	6.17	5.51
p8	0.46	0.51	0.58	0.64	0.71	0.78	0.94	1.10
Ethynyl Addition to the Middle Ethylenic Carbon (Starting from i13)								
Products	Collision Energy (kJ mol ⁻¹)							
	0	4.2	8.4	12.6	16.7	20.9	30.0	40.9
p7 from i11	88.73	89.64	90.37	90.99	91.53	91.90	92.58	92.94
p7 from i7	0.00	0.00	0.00	0.00	0.00	0.00	0.01	0.01
p7 total	88.73	89.64	90.37	90.99	91.53	91.90	92.59	92.95
p6 via i12	9.83	8.77	7.86	7.07	6.36	5.79	4.64	3.80
p6 via i7	0.91	0.99	1.07	1.15	1.23	1.31	1.51	1.69
p6 total	10.74	9.76	8.93	8.22	7.59	7.11	6.15	5.49
p8	0.53	0.60	0.69	0.78	0.88	0.99	1.26	1.56

conclusion that the rearrangement to **i2** (pathways (1) and (2), which is in agreement with the experimental observations. The final pathway (4) also results in a phenyl radical **i8** intermediate in which the deuterium atom is located in the meta position with respect to the radical center; this in turn leads to a hydrogen atom loss only. To summarize, ortho benzyne can be formed via pathways (1), (2), and (4), i.e., via an initial attack of the D1-ethynyl radical to the terminal carbon atoms of the acetylenic (1)/(2) or vinyl group (4).

We also conducted statistical calculations to predict theoretically the fractions of ortho benzyne synthesized. Table 2 shows RRKM product branching ratios calculated assuming that the reaction starts from different initial adducts, **i1** and **i14** (addition to acetylenic carbons) and **i11** and **i13** (additions to vinyl carbons). One can see that the acetylenic and vinyl additions are expected to result in rather different sets of products, but on the other hand, terminal and middle carbon additions in each case (**i1** versus **i14** and **i11** versus **i13**) give very similar product yields because **i14** \leftrightarrow **i1** and **i11** \leftrightarrow **i13** isomerizations occurring by ethynyl group migration are much faster than dissociation processes of these initial adducts. Ethynyl additions

to acetylenic products are computed to produce 91%–95% of hexa-1,2,3-triene-5-yne **p1** and 9%–5% of C₂H₃ + C₄H₂ at the high collision energy of 40.9 kJ mol⁻¹ used in the present experiment, with all other products giving insignificant contributions. At zero collision energy, the branching ratios slightly change to 97%–98% for **p1** and 2%–3% for C₂H₃ + C₄H₂. On the contrary, ethynyl additions to ethylenic carbons are calculated to form (Z)-hexa-3-ene-1,5-diyne **p7** as the major product (~93% at the collision energy of 40.9 kJ mol⁻¹ and ~89% at zero collision energy) and o-benzyne **p6** at fractions of 6% and 11% at collision energies of 40.9 and 0 kJ mol⁻¹, respectively, with trace amounts of diethynylethene **p8**. We may also conclude that the route from the reactants via **i11** \rightarrow **i7/i12** \rightarrow **i8** leads to D1-o-benzyne plus atomic hydrogen with the path via **i12** being more favorable. The preference of **p7** over o-benzyne owes to the “entropic” factor; even though the barrier for the direct H loss from **i11** is ~33 kJ mol⁻¹ higher than the highest in energy transition state on the **i11** \rightarrow **i12** \rightarrow **i8** \rightarrow **p6** route, the H loss transition state is looser than those for the ring closure and H migration on the o-benzyne formation route and therefore the number of states of the **i11** \rightarrow **p7** + H transition state is higher

and grows faster with the energy content. The branching in the entrance reaction channel (i.e., acetylenic versus ethylenic addition) can be addressed by sophisticated dynamics calculations since all addition pathways have no barrier. However, judging from a comparison of the rate constants for the ethynyl plus acetylene and ethynyl plus ethylene reactions, which are close to each other (Hebrard et al. 2009; Vakhtin et al. 2001a, 2001b), one can expect the ethynyl additions to the acetylenic and ethylenic carbons to occur with roughly equal probabilities. Therefore, the acyclic products **p1** and **p7** and o-benzyne with concentrations ranging from a few% to 10% at most can be predicted as the major products.

6. ASTROPHYSICAL IMPLICATIONS AND CONCLUSIONS

In recent years, small PAH molecules have been tentatively identified in comet 1P/Halley utilizing the three-channel spectrometer (TKS) on board the *Vega 2* spacecraft. These are phenanthrene (Moreels et al. 1994), pyrene (Clairemidi et al. 2004), and anthracene (Clairemidi et al. 2004). More recently, naphthalene, phenanthrene, and pyrene were identified in samples collected from comet 81P/Wilds during the stardust mission (Sandford et al. 2006). In interstellar environments, no individual PAH has been detected. Their simplest building block—the benzene molecule—has been tentatively identified in the protoplanetary nebula CRL-618 (Cernicharo et al. 2001). However, the transition from benzene to PAHs remains to be solved. Here, the o-benzyne molecule could play an important role (Frenklach & Feigelson 1989; Cherchneff et al. 1992). In this paper, we have provided evidence based on a combined crossed beam and electronic structure study that D1-substituted o-benzyne can be formed under single collision conditions in the gas-phase reaction of D1-ethynyl with vinylacetylene at a collision energy of 40.9 kJ mol⁻¹, which is roughly equal to about 4000 K as present in photospheres of carbon stars and protoplanetary nebulae close to the central star. The initial addition of D1-ethynyl to the terminal acetylenic and ethylenic carbon atoms of vinyl acetylene lead—via atomic hydrogen elimination—predominantly via the initial collision complexes **i1** and **i11** to two acyclic products, **p1** and **p7**. Based on the experiments and electronic structure calculations, ortho benzyne was also identified; computations predict branching ratios of up to 10%. Since the reaction has no barrier, the initial collision complexes **i1** and **i11**—a crucial prerequisite to form o-benzyne—is accessible even in cold clouds like TMC-1. Fueled by our assignment of o-benzyne as a reaction product, future theoretical work will investigate the temperature-dependent, absolute rate constants and the branching ratios of the o-benzyne versus non-aromatic isomers. These data can then be incorporated into refined models simulating the chemical evolution of distinct interstellar environments.

The experimental work and electronic structure calculations were supported by the chemistry division of the US National Science Foundation (NSF-CRC CHE-0627854).

REFERENCES

- Alajtal, A. I., Edwards, H. G. M., & Scowen, I. J. 2010, *Anal. Bioanal. Chem.*, 397, 215
- Allamandola, L. J., & Hudgins, D. M. 2003, in *Solid State Astrochemistry*, ed. V. Pirronello, J. Krelowski, & G. Monicò (NATO ASI Sci. Ser. II, 120; Dordrecht: Kluwer), 251
- Allamandola, L. J., Tielens, A. G. G. M., & Barker, J. R. 1985, *ApJ*, 290, L25
- Amos, R. D., et al. 2003, Molpro, Version 2002.6, A Package of ab initio Programs (Birmingham: Univ. Birmingham), <http://www.molpro.net>
- Balucani, N., Mebel, A. M., Lee, Y. T., & Kaiser, R. I. 2001, *J. Phys. Chem. A*, 105, 9813
- Becke, A. D. 1993, *J. Chem. Phys.*, 98, 5648
- Bockhorn, H., Fetting, F., Heddrich, A., & Wannemacher, G. 1987, *Ber. Bunsenges. Phys. Chem.*, 91, 819
- Cernicharo, J., Heras, A. M., Tielens, A. G. G. M., Pardo, J. R., Herpin, F., Guelin, M., & Waters, L. B. F. M. 2001, *ApJ*, 546, L123
- Chapman, O. L., Mattes, K., McIntosh, C. L., Pacansky, J., Calder, G. V., & Orr, G. 1973, *J. Am. Chem. Soc.*, 95, 6134
- Cherchneff, I., Barker, J. R., & Tielens, A. G. G. M. 1992, *ApJ*, 401, 269
- Clairemidi, J., Brechignac, P., Moreels, G., & Pautet, D. 2004, *Planet. Space Sci.*, 52, 761
- Cook, D. J., Schlemmer, S., Balucani, N., Wagner, D. R., Steiner, B., & Saykally, R. J. 1996, *Nature*, 380, 227
- Cox, N. L. J., et al. 2007, *A&A*, 465, 899
- Dunkin, I. R., & MacDonald, J. G. 1979, *J. Chem. Soc., Chem. Commun.*, 772
- Dunning, T. H., Jr 1989, *J. Chem. Phys.*, 90, 1007
- Frenklach, M., & Feigelson, E. D. 1989, *ApJ*, 341, 372
- Frisch, M. J., et al. 2001, Gaussian 98, Revision A5 (Pittsburgh, PA: Gaussian, Inc.)
- Gu, X., Guo, Y., Chan, H., Kawamura, E., & Kaiser, R. I. 2005a, *Rev. Sci. Instrum.*, 76, 116103/1
- Gu, X., Guo, Y., & Kaiser, R. I. 2005b, *Int. J. Mass Spectrosc.*, 246, 29
- Gu, X., Guo, Y., Mebel, A. M., & Kaiser, R. I. 2007, *Chem. Phys. Lett.*, 449, 44
- Gu, X., Guo, Y., Zhang, F., Mebel, A. M., & Kaiser, R. I. 2006, *Faraday Discuss.*, 133, 245
- Guo, Y., Gu, X., & Kaiser, R. I. 2006a, *Int. J. Mass Spectrom. Ion Phys.*, 249, 420
- Guo, Y., Gu, X., Kawamura, E., & Kaiser, R. I. 2006b, *Rev. Sci. Instrum.*, 77, 034701/1
- Guo, Y., Gu, X., Zhang, F., Mebel, A. M., & Kaiser, R. I. 2007, *Phys. Chem. Chem. Phys.*, 9, 1972
- Halasinski, T. M., Salama, F., & Allamandola, L. J. 2005, *ApJ*, 628, 555
- Hebrard, E., et al. 2009, *J. Phys. Chem. A*, 113, 11227
- Hudgins, D. M., Bauschlicher, C. W., Jr., & Allamandola, L. J. 2005, *ApJ*, 632, 316
- Huh, S. B., & Lee, J. S. 2003, *J. Chem. Phys.*, 118, 3035
- Jackson, W. M., & Scodinu, A. 2004, *Astrophys. Space Sci. Libr.*, 311, 85
- Joblin, C., Berne, O., Simon, A., & Mulas, G. 2009, in *ASP Conf. Ser. 414, Cosmic Dust—Near and Far*, ed. T. Henning, E. Grün, & J. Steinacker (San Francisco, CA: ASP), 383
- Kaiser, R. I., Balucani, N., Charkin, D. O., & Mebel, A. M. 2003, *Chem. Phys. Lett.*, 382, 112
- Kaiser, R. I., Oschsenfeld, C., Head-Gordon, M., Lee, Y. T., & Suits, A. G. 1996, *Science*, 274, 1508
- Kaiser, R. I., et al. 2010, *Faraday Discuss.*, 147, 429
- Kislov, V. V., Nguyen, T. L., Mebel, A. M., Lin, S. H., & Smith, S. C. 2004, *J. Chem. Phys.*, 120, 7008
- Kraka, E., & Cremer, D. 1993, *Chem. Phys. Lett.*, 216, 333
- Kukulich, S. G., McCarthy, M. C., & Thaddeus, P. 2004, *J. Phys. Chem. A*, 108, 2645
- Lee, C., Yang, W., & Parr, R. G. 1988, *Phys. Rev. B*, 37, 785
- Leger, A., & Puget, J. L. 1984, *A&A*, 137, L5
- Levine, R. D. 2005, *Molecular Reaction Dynamics* (Cambridge: Cambridge Univ. Press)
- Matimba, H. E. K., Crabbendam, A. M., Ingemann, S., & Nibbering, N. M. M. 1991, *J. Chem. Soc., Chem. Commun.*, 9, 644
- McMahon, R. J., McCarthy, M. C., Gottlieb, C. A., Dudek, J. B., Stanton, J. F., & Thaddeus, P. 2003, *ApJ*, 590, L61
- Mebel, A. M., Kislov, V. V., & Kaiser, R. I. 2008, *J. Am. Chem. Soc.*, 130, 13618
- Mebel, A. M., Lin, M. C., Chakraborty, D., Park, J., Lin, S. H., & Lee, Y. T. 2001, *J. Chem. Phys.*, 114, 8421
- Meier, M. S., Wang, G.-W., Haddon, R. C., Brock, C. P., Lloyd, M. A., & Selegue, J. P. 1998, *J. Am. Chem. Soc.*, 120, 2337
- Miller, W. B., Safron, S. A., & Herschbach, D. R. 1967, *Discuss. Faraday Soc.*, 44, 108
- Moreels, G., Clairemidi, J., Hermine, P., Brechignac, P., & Rousselot, P. 1994, *A&A*, 282, 643
- Onaka, T. 2004, in *ASP Conf. Ser. 309, Astrophysics of Dust*, ed. A. N. Witt, G. C. Clayton, & B. T. Draine (San Francisco, CA: ASP), 163
- Onaka, T., Kaneda, H., Sakon, I., & Matsumoto, H. 2009, in *ASP Conf. Ser. 414, Cosmic Dust—Near and Far*, ed. T. Henning, E. Grün, & J. Steinacker (San Francisco, CA: ASP), 227

- Peeters, E., Hony, S., Van Kerckhoven, C., Tielens, A. G. G. M., Allamandola, L. J., Hudgins, D. M., & Bauschlicher, C. W. 2002, *A&A*, **390**, 1089
- Peterson, K. A., & Dunning, T. H., Jr. 1995, *J. Phys. Chem.*, **99**, 3898
- Phillips, S. J. M., & Parnell, J. 2006, *Int. J. Astrobiol.*, **5**, 353
- Pople, J. A., Head-Gordon, M., & Raghavachari, K. 1987, *J. Chem. Phys.*, **87**, 5968
- Purvis, G. D., III, & Bartlett, R. J. 1982, *J. Chem. Phys.*, **76**, 1910
- Radziszewski, J. G., Hess, B. A., Jr., & Zahradnik, R. 1992, *J. Am. Chem. Soc.*, **114**, 52
- Robertson, E. G., Godfrey, P. D., & McNaughton, D. 2003, *J. Mol. Spectrosc.*, **217**, 123
- Rosenstock, H. M., Stockbauer, R., & Parr, A. C. 1980, *J. Chim. Phys. Phys.-Chim. Biol.*, **77**, 745
- Sakon, I., Onaka, T., Ishihara, D., Ootsubo, T., Yamamura, I., Tanabe, T., & Roellig, T. L. 2004, *ApJ*, **609**, 203
- Sandford, S. A., et al. 2006, *Science*, **314**, 1720
- Sarre, P. J. 2006, *J. Mol. Spectrosc.*, **238**, 1
- Scuseria, G. E., Janssen, C. L., & Schaefer, H. F., III 1988, *J. Chem. Phys.*, **89**, 7382
- Scuseria, G. E., & Schaefer, H. F., III 1989, *J. Chem. Phys.*, **90**, 3700
- Shukla, B., Susa, A., Miyoshi, A., & Koshi, M. 2008, *J. Phys. Chem. A*, **112**, 2362
- Tielens, A. G. G. M. 2008, *ARA&A*, **46**, 289
- Vakhtin, A. B., Heard, D. E., Smith, I. W. M., & Leone, S. R. 2001a, *Chem. Phys. Lett.*, **344**, 317
- Vakhtin, A. B., Heard, D. E., Smith, I. W. M., & Leone, S. R. 2001b, *Chem. Phys. Lett.*, **348**, 21
- Vernon, M. 1981, PhD thesis, Univ. California, Berkeley
- Weiss, M. S. 1986, PhD thesis, Univ. California, Berkeley
- Wenthold, P. G., Hu, J., & Squires, R. R. 1996, *J. Am. Chem. Soc.*, **118**, 11865
- Wentrup, C., Blanch, R., Briehl, H., & Gross, G. 1988, *J. Am. Chem. Soc.*, **110**, 1874
- Widicus Weaver, S. L., Remijan, A. J., McMahon, R. J., & McCall, B. J. 2007, *ApJ*, **671**, L153
- Wodtke, A. M., & Lee, Y. T. 1985, *J. Phys. Chem.*, **89**, 4744
- Zhang, F., Jones, B., Maksyutenko, P., Kaiser, R. I., Chin, C., Kislov, V. V., & Mebel, A. M. 2010, *J. Am. Chem. Soc.*, **132**, 2672
- Zhang, F., Kim, S., Kaiser, R. I., & Mebel, A. M. 2009, *J. Phys. Chem. A*, **113**, 1210
- Zhang, X., & Chen, P. 1992, *J. Am. Chem. Soc.*, **114**, 3147
- Zhang, X., et al. 2007, *J. Chem. Phys.*, **126**, 044312/1